SUPPLEMENTAL MATERIAL

EXPERIMENTAL METHODS

Data Analysis

Data were analyzed off-line by measuring the changes in maximum diastolic potentials and AP duration (MDP and APD) during triggered waves. Mean fluorescence was calculated as the average along each line of the linescan image and included with the figures to show changes in overall Ca2+ during the linescan. Changes in membrane voltage (ΔVm) were measured using pCLAMP 8 software while Ca2+ (ΔCa2+) was measured in the standard manner using ΔF/F0 so that absolute changes could be measured during rapid pacing. F0 was measured as diastolic Ca2+ fluorescence at steady state during pacing but before the first AP of triggered wave occurrence at each pacing rate. The change in Vm/MDP during a triggered wave was calculated by measuring the difference in MDP between the last beat before the wave and the MDP from which the AP was initiated during the TCW (see Figure S1 for diagram). Data were plotted and fitted to linear relationships for ΔVm vs. ΔF/F0 and the slope of this relationship was calculated in the absence and presence of NCX block in order to determine the role of inward NCX current (I_{NCX}) on changes in MDP and APD during triggered waves. APD changes were measured as the difference between the AP during which a wave occurred compared to the previous unaffected AP at the same pacing rate.

The number of AP cycles affected by the triggered wave was calculated as shown in Figure 2B. The beginning of the triggered wave occurred during the cycle indicated by the vertical line labelled F0, continued through cycles labelled F1, F2, F3 and ended at the beginning of F4. Therefore, 4 cycles were affected by the triggered wave: APs F0-F1, F1-F2, F2-F3 and F3-F4.

APD was calculated as shown in Figure 3A as the difference in APD at -20 and -50mV during repolarization (APD-20, APD-50) between successive pairs of APs in the absence and presence of a triggered wave. The difference between APD-20 and APD-50 are shown in Figure 4B. Horizontal lines indicate where APD50 and APD 90 were measured in a cycle without a triggered wave followed by a cycle with a wave as indicated by the mean fluorescence shown below the Vm recording. It did not matter if the wave occurred during the first or the second cycle for the paired calculation.

Statistics

All statistical comparisons were made using paired or unpaired t-tests or an analysis of variance with appropriate post hoc pairwise comparisons. Data were obtained from a minimum of 3 dogs for all data described in this study with the exception of some additional data obtained with a second NCX inhibitor, ORM10103, where data are included for the purpose of confirming the more complete data set obtained with SEA0400. In this case, results were obtained from only 2 dogs so no attempt was made to perform statistics on these data and all original data for each experiment are presented in the Supplementary Material in Figure S1 (see below). A difference between sample means was considered significant if $p<0.05$.

MODELING METHODS

Cell model

In this study we apply our recently developed phenomenological model of triggered waves (TCWs) in atrial myocytes[1-3] in order to explore how these Ca2+ release events affect cardiac tissue. In this model we account for the number of Ca2+ sparks recruited at: (i) Junctional sites near the cell boundary where LCC and RyR clusters are in close proximity. Here, Ca2+ sparks

are initiated by LCC channel openings, and the local Ca2+ release is graded with respect to the whole cell I_{Ca}. (ii) Non-junctional sites in the cell interior, where RyR clusters are isolated and open only due to Ca2+ that diffuses from a neighboring cluster, or due to intrinsic RyR channel gating. By accounting for the stochastic recruitment of these two populations of clusters we are able to model the key dynamical features of TCWs. Using this model we have shown previously that the intermittent large increases of intracellular Ca2+ observed in our experiments are due to Ca2+ waves triggered at junctional sites which proceed to activate non-junctional sites via propagating Ca2+ waves.

In this approach, we model Ca2+ cycling phenomenologically by keeping track only of the number of Ca2+ sparks in the cell. To model Ca2+ release we denote $n_i(t)$ to be the number of non-junctional sites at which Ca2+ is being released due to a Ca2+ spark at time t. Similarly, we count the number of sparks at junctional sites denoted as $n_b(t)$. Ca2+ sparks are formed and extinguished in their respective volumes according to the reaction scheme

$$0 \underset{\beta_i}{\overset{\alpha_i}{\rightleftharpoons}} 1 \ , \tag{1}$$

$$0 \underset{\beta_b}{\overset{\alpha_b}{\rightleftharpoons}} 1 \ , \tag{2}$$

where 0 denotes an "off" cluster which is shut and 1 denotes an "on" cluster at which Ca2+ is being released due to a spark. The rate at which Ca2+ sparks are activated at non-junctional and junctional clusters is given by α_i and α_b respectively, and with corresponding extinction rates β_i and β_b. Time evolution of the number of sparks at N_i non-junctional Ca2+ release units (CRUs) is modelled according to

$$n_i(t + \Delta t) = n_i(t) + \Delta n_i^+ - \Delta n_i^-, \tag{3}$$

where

$$\Delta n_i^+ = B(\alpha_i \Delta t, N_i - n_i), \tag{4}$$

$$\Delta n_i^- = B(\beta_i \Delta t, n_i), \tag{5}$$

and where $B(p, n)$ is a random number picked from a binomial distribution with success probability p and number of trials n. Time evolution of the number of junctional sparks n_b is modelled in a similar fashion.

To model triggered waves using this approach we apply a phenomenological approach and write the spark recruitment rate as a function of the main Ca2+ cycling variables. Thus, the rate of spark recruitment at non-junctional sites is taken to have the functional form

$$\alpha_i = \big(a_i F(p_b) + b_i G(p_i)\big)\phi\big(c_{jsr}\big), \tag{6}$$

where a_i and b_i are adjustable constants. Here, p_b denotes the fraction of sparks at junctional sites, and p_i denotes the fraction of sparks at non-junctional sites. Therefore, the non-junctional spark rate is governed by the functions $F(p_b), G(p_i)$ and $\phi(c_{jsr})$, which gives the dependence on p_b, p_i, and the SR load c_{jsr}. To model wave nucleation we use a sigmoid dependence given by

$$F(p_b) = \frac{1}{1 + \left(\frac{p_b^*}{p_b}\right)^{\gamma_b}} \tag{7}$$

where p_b^* is the threshold for wave activation. In this way, the rate at which Ca2+ sparks are recruited at non-junctional sites is dependent on the fraction of sparks recruited at junctional sites. Thus, a reduction in the threshold p_b^* makes the cell interior more prone to initate Ca2+ waves. Model parameters used are identical to that used in our previous publication[3].

To model TCW coupling to Vm, we coupled Ca2+ cycling to the major ion currents developed in the Grandi et al[4] model of the human atrial myocyte. In particular we incorporate their ionic current formulations for the fast Na+ current (I_{Na}), the rapidly activating delayed rectifier K^+ current (I_{Kr}), the slowly activating delayed rectifier K^+ current (I_{Ks}), the ultra-rapid delayed rectifier K^+ current

(I_{Kur}), the inward rectifier K^+ current (I_{K1}) , the transient outward K^+ current (I_{to}), the Na^+/K^+ pump current (I_{NaK}), and finally the NCX current (I_{NCX}). To model the voltage time course observed in response to triggered waves, we have decreased the conductance of I_{K1} by 50%.

Tissue modeling

To model electrical propagation we apply the cable equation

$$\frac{\partial V}{\partial t} = -\frac{I_{ion}}{C_m} + D_V\left(\frac{\partial^2 V}{\partial x^2} + \frac{\partial^2 V}{\partial y^2}\right)$$

where $C_m = 1\mu F/cm^2$ is the membrane capacitance, $D_V = 5 \times 10^{-3} cm^2/ms$ is the effective voltage diffusion coefficient, and I_{ion} is the total transmembrane current. The cable equation is integrated using an operator splitting approach with a space step $\Delta x = 0.015cm$ and with a variable time step in the range $dt = 0.01 - 0.1ms$[5].

SUPPLEMENTARY DATA

Calculation of Change in Vm during TCWs

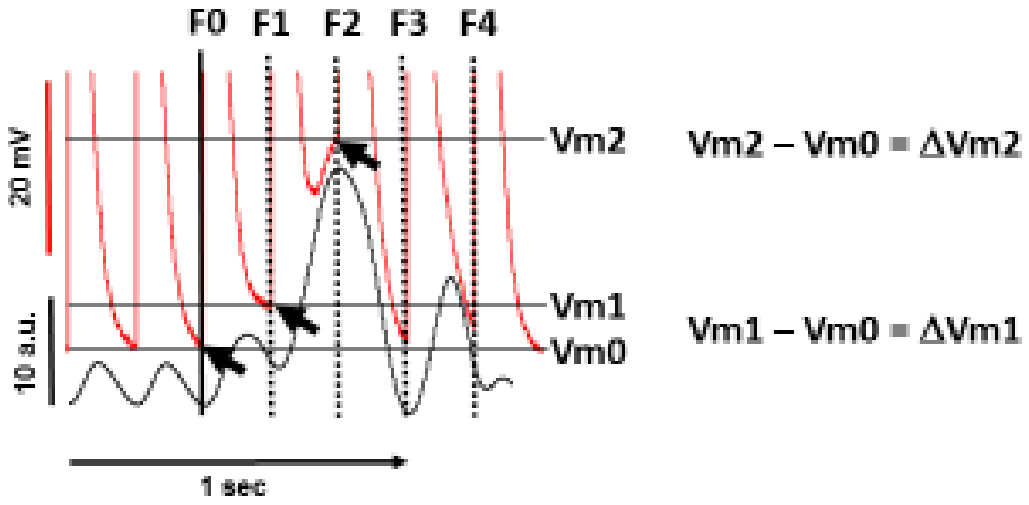

Figure S1. Method for calculation of ΔVm during TCWs. F0 indicates the initiation of the last AP activated before the beginning of the TCW. F1 is the next AP activated early during the TCW and F2 was activated nearly at the peak of the TCW. Values for Vm indicate Maximum Diastolic Potential (MDP) for each response are indicated as Vm0, Vm1 and Vm2, respectively. ΔVm was calculated as the difference between MDP during the TCW and MDP of the last AP before the TCW (F0, VM0).

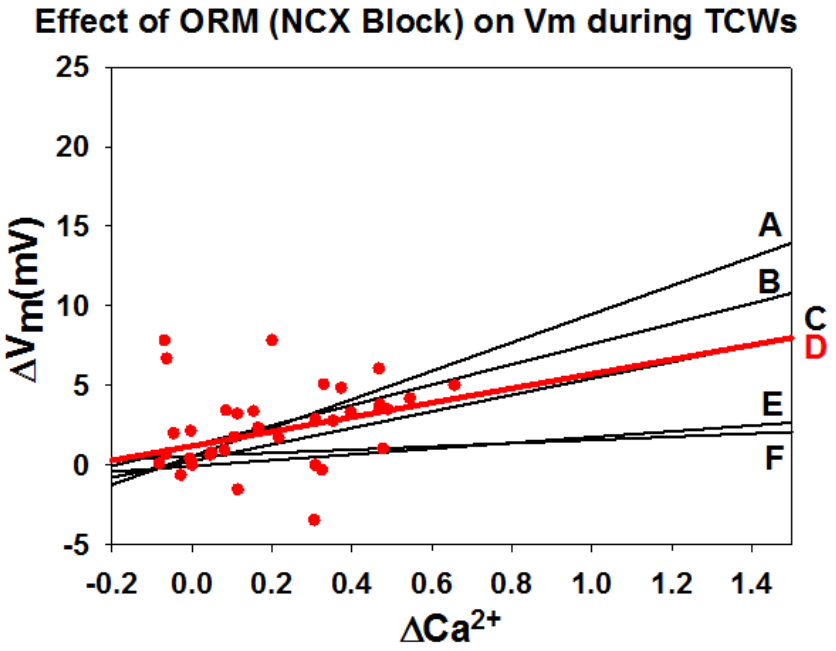

Figure S2. Inhibition of depolarization of maximum diastolic potential by triggered Ca2+ waves. The results were obtained in 6 cells from 2 dog atria and each line shows the linear fit to the data for each experiment. The red points and the accompanying red line show the results from a representative experiment (D). Individual data points were omitted for the other experiments for the sake of clarity of the figure (lines A,B,C,E,F).

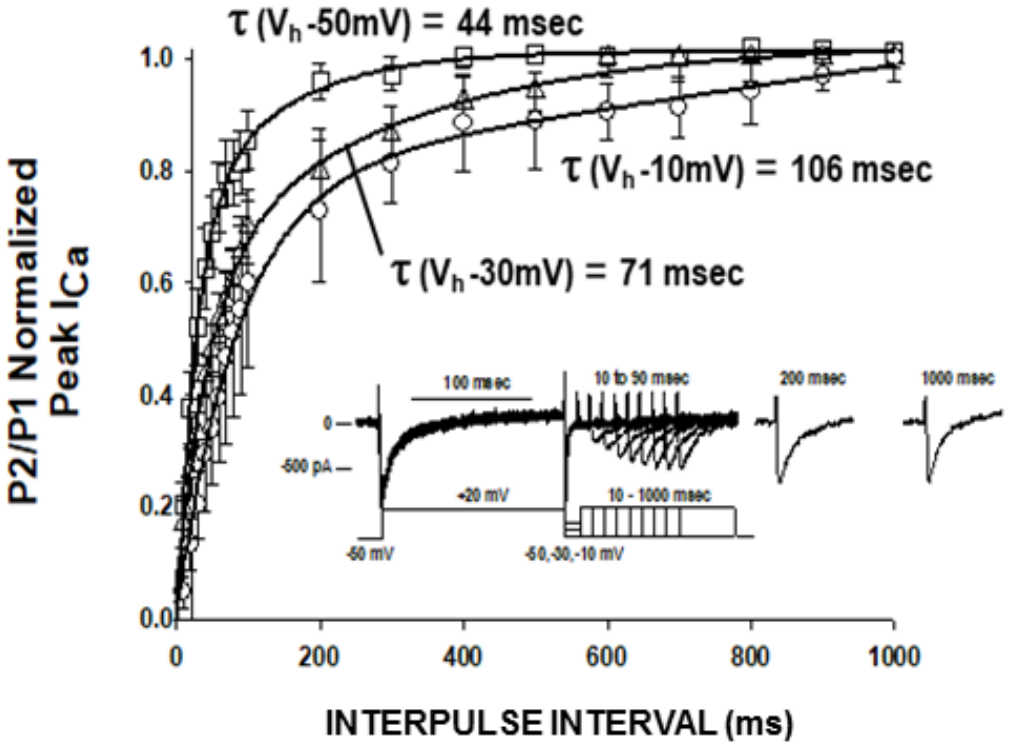

Figure S3. Voltage dependence of recovery from inactivation of I_{Ca} in atrial myocytes.

The inset shows both the protocol and the original recordings from an experiment where holding potential (Vh) = -50mV. Graphed summary data were derived from the number of myocytes as follows: Vh=-50mV, n=10 (6 dogs); Vh=-30mV (7 dogs), n=8; Vh=-10mV, n=4 (3 dogs).

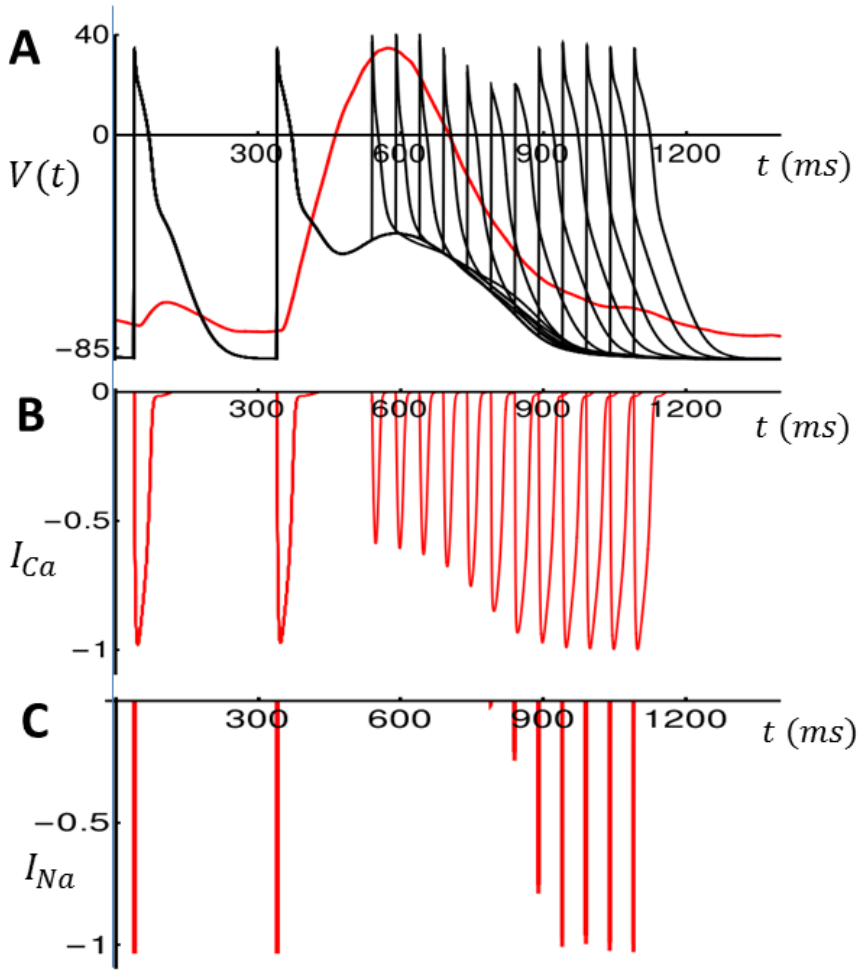

Figure S4. Simulation of Ca2+ and Na+ currents during the AP.

(A) AP response during a TCW. The black line denotes $V(t)$ for 12 simulation runs where the last stimulations occurs over a range of CLs ranging from 800ms to 200ms. In this simulation, the underlying Ca2+ concentration is clamped and exhibits a TCW (red line). (B) I_{Ca} for each simulation run. (C) I_{Na} for each simulation run. In both cases, currents are normalized to the maximum current measured during the first 2 beats.

References:

1. Aistrup GL, Arora R, Grubb S, Yoo S, Toren B, Kumar M, Kunamalla A, Marszalec W, Motiwala T, Tai S, Yamakawa S, Yerrabolu S, Alvarado FJ, Valdivia HH, Cordeiro JM, Shiferaw Y and Wasserstrom JA. Triggered intracellular calcium waves in dog and human left atrial myocytes from normal and failing hearts. *Cardiovascular research*. 2017;113:1688-1699.
2. Shiferaw Y, Aistrup GL and Wasserstrom JA. Mechanism for Triggered Waves in Atrial Myocytes. *Biophysical journal*. 2017;113:656-670.
3. Shiferaw Y, Aistrup GL and Wasserstrom JA. Synchronization of Triggered Waves in Atrial Tissue. *Biophysical journal*. 2018;115:1130-1141.
4. Grandi E, Pandit SV, Voigt N, Workman AJ, Dobrev D, Jalife J and Bers DM. Human atrial action potential and Ca2+ model: sinus rhythm and chronic atrial fibrillation. *Circ Res*. 2011;109:1055-66.
5. Qu Z and Garfinkel A. An advanced algorithm for solving partial differential equation in cardiac conduction. *IEEE Trans Biomed Eng*. 1999;46:1166-8.